Proceedings of the XII International Symposium on Dynamic Problems of Mechanics (DINAME 2007),
P.S.Varoto and M.A.Trindade (editors), ABCM, Ilhabela, SP, Brazil, February 26 - March 2, 2007

Magneto-Rheological Vehicle Suspension System based on the Variable Structure Control applied to a Flexible Half-Vehicle Model

Leonardo Tavares Stutz[1] **and Fernando Alves Rochinha**[2]

[1] Universidade Estadual do Rio de Janeiro, Instituto Politécnico
PO Box 97.282, Zip Code 28610-974, Nova Friburgo, RJ, Brazil
ltstutz@iprj.uerj.br

[2] Universidade Federal do Rio de Janeiro, COPPE/PEM
PO Box 68.503, Zip Code 21945-970, Rio de Janeiro, RJ, Brasil
faro@adc.coppe.ufrj.br

Abstract: The synthesis of a magneto-rheological vehicle suspension system based on the Variable Structure Control approach is presented in this work. A half-vehicle model with rigid body was considered for the suspension synthesis. A reference model based on the vehicle nominal model was considered for specifying the desired dynamics for the vehicle body and a control force was derived in order to force the tracking error dynamics, between the state of the vehicle body and that of the reference model, to attain a sliding mode. To induce the MR dampers to approximately reproduce the desired variable structure control force, the input voltages to their current drivers were derived according to the Clipped-Control algorithm. The steady-state and transient performances of the suspension were assessed through numerical analyses. Despite not have been considered for the synthesis of the suspension, phenomenological models for the MR dampers and for the seat-driver subsystem along with a half-vehicle model with flexible body were considered for the performance assessment. For comparison purposes, a MR suspension based on the Optimal Control approach and two ideal active suspensions were also considered.

Keywords: Magneto-Rheological Suspension, Variable Structure Control, Flexible Half-Vehicle, Seat-Driver Subsystem.

INTRODUCTION

The aggressive competition within the Automobile Industry, along with the tightening of the requirements on human safety and comfort, has yield to the need of improving the vehicle suspension systems. The developing coming from this scenario aim at very different targets ranging from ride comfort to safety, passing through road damage minimization. They constitute complex and not necessarily harmonic goals to be achieved, given rise to significant technological challenges.

Three main strategies can be considered for vehicle suspension, namely: passive, active and semi-active. Usually, passive suspensions are effective only in a limited range of the vehicle operation. Conflicting trade-offs between different performance indices, such as ride comfort and road holding, are extremely difficult to be achieved with passive suspensions (Sharp and Hassan, 1986). Much more flexible and, consequently, more effective systems can be obtained relying upon the use of active suspensions (Hrovat, 1997). Although these suspensions present an improvement on the the capacity of the vehicle to adapt to changes in the operation conditions, they often require excessive power supply and sophisticated electronic devices not compatible with the industry standards. In order to circumvent these technical barriers, a lot of effort has been recently devoted to semi-active suspensions (Yao et al., 2002; Yokoyama et al., 2001; Stutz and Rochinha, 2005). Essentially, semi-active suspensions have properties that can be dynamically changed in order to optimally achieve the goals. The Semi-active systems represent one of the most promising devices for practical applications in vibration isolation problems. This is due to their inherent stability and versatility, besides the relative simplicity and much lower power demand as compared with their active counterparts (Carlson and Spencer, 1996).

The development of the electro-rheological and magneto-rheological (MR) dampers increased the applicability of the semi-active suspensions. In these devices, the viscosity of the fluids can be dramatically changed in the presence of electric and magnetic fields, respectively. However, these systems present highly nonlinear dynamic behavior and one of the main challenges in the application of MR suspensions is the development of appropriate control algorithms (Jansen and Dyke, 1999; Stutz and Rochinha, 2005).

In the present work, a MR suspension system is synthesized built on the Variable Structure Control approach (Edwards and Spurgeon, 1998). The suspension synthesis was developed as follows (Stutz, 2005). A reference model based on the vehicle nominal model was considered for specifying the desired dynamics for the vehicle body and a control force was derived in order to force the tracking error dynamics, between the state of the vehicle body and that of the reference model, to attain a sliding mode. To induce the MR dampers to approximately reproduce the desired variable structure control force, the input voltages to their current drivers were derived according to the Clipped-Control algorithm (Jansen and

Dyke, 1999). The inherent robustness of the variable structure control is required to deal with parameters uncertainties commonly present in the vehicle model.

The steady-state and transient performances of the suspension were assessed through numerical analyses, where phenomenological models for the MR dampers and for the seat-driver subsystem, along with a half-vehicle model with flexible body, were taken into account. It will be shown that, due to the control-structure interaction, accounting for the flexibility of the vehicle body, in the performance assessment of active and MR suspensions systems, is a fundamental concern. Besides, the performance of the MR dampers are greatly dependent on the control approach, the intensity of the vehicle body and the vehicle model considered.

MATHEMATICAL MODELING

Half-Vehicle Model with Rigid Body

The present work considers a half-vehicle model with rigid body, depicted in Fig. 1, for the synthesis of a magneto-rheological (MR) vehicle suspension system. In this model, the vehicle posses a rigid body of mass m_1 and moment of inertia J_{CG}. The masses m_{1f} and m_{1r} represent the effective ones of the front and rear suspensions, respectively. The suspensions are composed of springs k_{1f} and k_{1r}; dampers d_{1f} and d_{1r}; and control elements u_f and u_r.

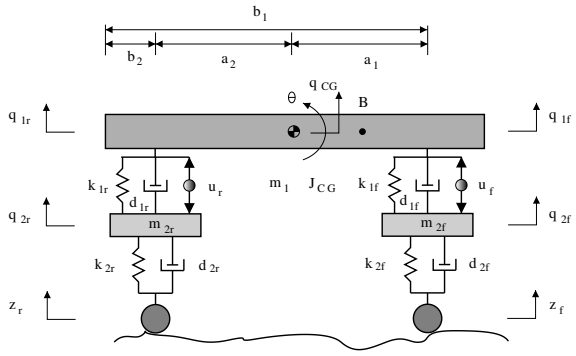

Figure 1 – Half-vehicle model with rigid body.

The dynamic behavior of the half-vehicle model is given by the equations

$$\begin{aligned}
&m_1\ddot{q}_{CG} + d_{1f}(\dot{q}_{1f} - \dot{q}_{2f}) + d_{1r}(\dot{q}_{1r} - \dot{q}_{2r}) + k_{1f}(q_{1f} - q_{2f}) + k_{1r}(q_{1r} - q_{2r}) = u_f + u_r \\
&J_{CG}\ddot{\theta} + a_1 d_{1f}(\dot{q}_{1f} - \dot{q}_{2f}) - a_2 d_{1r}(\dot{q}_{1r} - \dot{q}_{2r}) + a_1 k_{1f}(q_{1f} - q_{2f}) - a_2 k_{1r}(q_{1r} - q_{2r}) = a_1 u_f - a_2 u_r \\
&m_{2f}\ddot{q}_{2f} + d_{2f}\dot{q}_{2f} + d_{1f}(\dot{q}_{2f} - \dot{q}_{1f}) + k_{2f}q_{2f} + k_{1f}(q_{2f} - q_{1f}) = -u_f + d_{2f}\dot{z}_f + k_{2f}z_f \\
&m_{2r}\ddot{q}_{2r} + d_{2r}\dot{q}_{2r} + d_{1r}(\dot{q}_{2r} - \dot{q}_{1r}) + k_{2r}q_{2r} + k_{1r}(q_{2r} - q_{1r}) = -u_r + d_{2r}\dot{z}_r + k_{2r}z_r
\end{aligned} \tag{1}$$

where $(\cdot)$ is the differentiation with respect to time, q_{CG} is the vertical displacement of the center of gravity CG, θ is the angular displacement of the vehicle body, q_{1f} and q_{1r} are the vertical displacements of the connection points between the vehicle body and the front and rear suspensions, respectively; q_{2f} and q_{2r} are the displacements of the front and rear wheels; and z_f e z_r are front and rear disturbances due to the movement of the vehicle over an unevenness road.

Defining the generalized displacement vector $\mathbf{q}^T$=$[q_{CG} \quad \theta \quad q_{2f} \quad q_{2r}]$, Eq. (1) may be written in the matrix form

$$\dot{\mathbf{x}} = \mathbf{A}\mathbf{x} + \mathbf{B}\mathbf{u} + \mathbf{B}_{fz}\mathbf{f}_z \tag{2}$$

where the state vector $\mathbf{x}$, the control action $\mathbf{u}$ and the disturbance $\mathbf{f}_z$ are defined as follow

$$\mathbf{x} = \begin{bmatrix} \mathbf{q} \\ \dot{\mathbf{q}} \end{bmatrix} \quad ; \quad \mathbf{u} = \begin{bmatrix} u_f \\ u_r \end{bmatrix} \quad ; \quad \mathbf{f}_z = \begin{bmatrix} d_{2f}\dot{z}_f + k_{2f}z_f \\ d_{2r}\dot{z}_r + k_{2r}z_r \end{bmatrix} \tag{3}$$

Magneto-Rheological Damper

In order to model the nonlinear behavior of the MR damper, the modified Bouc-Wen model depicted in Fig. 2 is adopted in this work. This model has been shown to accurately predict the nonlinear behavior of a prototype MR damper over a wide range of inputs (Spencer et al., 1996).

In the modified Bouc-Wen model, the force generated by the MR damper is given by

$$u = c_1\dot{y} + k_1(q - q_0) \tag{4}$$

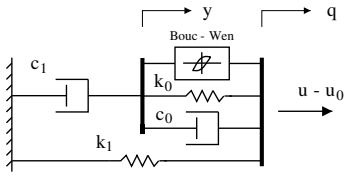

Figure 2 – The modified Bouc-Wen model of the MR damper.

where the internal variable y and the hysteretic displacement h are given by the following equations

$$\dot{y} = \frac{1}{(c_0+c_1)}[\alpha h + c_0\dot{q} + k_0(q-y)] \qquad ; \qquad \dot{h} = -\gamma|\dot{q}-\dot{y}|h|h|^{n-1} - \beta(\dot{q}-\dot{y})|z|^n + \mathscr{A}(\dot{q}-\dot{y}) \tag{5}$$

where the parameters γ, β, $\mathscr{A}$ and n control the shape of the hysteresis loop. The model parameters are assumed to be dependent on the voltage V applied to the current driver as follows

$$\alpha(v) = \alpha_a + \alpha_b v \qquad ; \qquad c_1(v) = c_{1a} + c_{1b} v \qquad ; \qquad c_0(v) = c_{0a} + c_{0b} v \tag{6}$$

where v is the output of the first order filter that accounts the dynamics involved in reaching the rheological equilibrium, viz.

$$\dot{v} = -\frac{1}{\tau}(v - V) \tag{7}$$

Seat-Driver Subsystem

In the present work, a MR suspension based on the Variable Structure Control will be synthesized in order to improve on the ride comfort obtained by the passive suspension system. Therefore, a phenomenological model of the seat-driver subsystem, depicted in Fig. 3, will be considered for performance assessment. This model presents an apparent mass similar to that of seated human body exposed to vertical vibrations (Wei and Griffin, 1998). In Fig. 3, the seat is modeled by the spring k_{d1} and the damper d_{d1}; the point C represents the driver position and the point B is the connection point between the vehicle body and the seat-driver subsystem (see Fig. 1).

The dynamic behavior of the seat-drive subsystem is given by

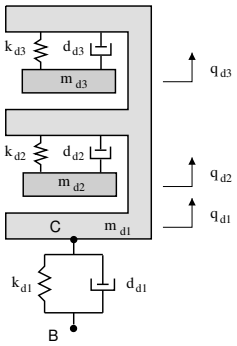

Figure 3 – Phenomenological model of the seat-driver subsystem.

$$\begin{aligned} &m_{d1}\ddot{q}_{d1} + d_{d1}(\dot{q}_{d1}-\dot{q}_B) + d_{d2}(\dot{q}_{d1}-\dot{q}_{d2}) + d_{d3}(\dot{q}_{d1}-\dot{q}_{d3}) + \\ &\qquad + k_{d1}(q_{d1}-q_B) + k_{d2}(q_{d1}-q_{d2}) + k_{d3}(q_{d1}-q_{d3}) = 0 \\ &m_{d2}\ddot{q}_{d2} + d_{d2}(\dot{q}_{d2}-\dot{q}_{d1}) + k_{d2}(q_{d2}-q_{d1}) = 0 \\ &m_{d3}\ddot{q}_{d3} + d_{d3}(\dot{q}_{d3}-\dot{q}_{d1}) + k_{d3}(q_{d3}-q_{d1}) = 0 \end{aligned} \tag{8}$$

MR-VSC VEHICLE SUSPENSION SYSTEM

The MR-VSC suspension was synthesized as follows. A reference model was considered for specifying the desired dynamics for the vehicle body and a control force was derived, built on the VSC, in order to force the tracking error dynamics, between the state vector of the vehicle body and that of the reference model, to attain a sliding mode (Yokoyama et al., 2001). This force was taken as the desired control force u_d for the MR damper. Then, the Clipped-Control approach (Jansen and Dyke, 1999) was considered for determining an input voltage V to the current driver of the MR damper in order that the generated force u approximately reproduces the desired one.

The dynamic behavior of the vehicle body, described by the first two equations in Eq. (1), may be written in the more general state-space form as

$$\dot{\mathbf{x}}_b = \mathbf{A}_b\mathbf{x}_b + \mathbf{B}_b\left(\mathbf{u} + \mathbf{f}_2 + \mathbf{f}_p + \mathbf{f}_\phi\right) \tag{9}$$

where the state vector of the vehicle body $\mathbf{x}_b$ and the signal $\mathbf{f}_2$ are defined as

$$\mathbf{x}_b^T = \begin{bmatrix} q_{CG} & \theta & \dot{q}_{CG} & \dot{\theta} \end{bmatrix} \qquad \mathbf{f}_2 = \begin{bmatrix} d_{1f}\dot{q}_{2f} + k_{1f}q_{2f} \\ d_{1r}\dot{q}_{2r} + k_{1r}q_{2r} \end{bmatrix} \tag{10}$$

It is worth noting that the signal $\mathbf{f}_2$ is defined from nominal parameters and the wheel dynamics, which is considered as known. The signal $\mathbf{f}_\phi$ accounts for matched disturbances (Edwards and Spurgeon, 1998) resulting from unmodeled dynamics, i.e., the ones resulting from the flexibility of the vehicle body. The signal $\mathbf{f}_p$ accounts for parameter uncertainties and is given by

$$\mathbf{f}_p = \begin{bmatrix} -\Delta d_{1f}(\dot{q}_{1f} - \dot{q}_{2f}) - \Delta k_{1f}(q_{1f} - q_{2f}) - \left(\frac{a_2\Delta m_1\ddot{q}_{CG} + \Delta J_{CG}\ddot{\theta}}{a_1 + a_2}\right) \\ -\Delta d_{1r}(\dot{q}_{1r} - \dot{q}_{2r}) - \Delta k_{1r}(q_{1r} - q_{2r}) - \left(\frac{a_1\Delta m_1\ddot{q}_{CG} - \Delta J_{CG}\ddot{\theta}}{a_1 + a_2}\right) \end{bmatrix} \tag{11}$$

where $\Delta(\cdot)$ represents the uncertainty on the nominal parameter $(\cdot)$.

Synthesis of the Reference Model

In order to specify the desired dynamics for the vehicle body, the reference model depicted in Fig. 4 was adopted.

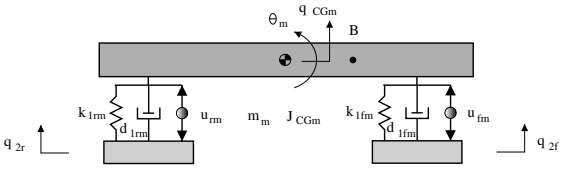

Figure 4 – Reference model for the vehicle body.

The dynamics of the reference model is given by

$$\dot{\mathbf{x}}_{bm} = \mathbf{A}_{bm}\mathbf{x}_{bm} + \mathbf{B}_{bm}\left(\mathbf{u}_m + \mathbf{f}_{2m}\right) \tag{12}$$

where the state vector $\mathbf{x}_{bm}$ and the signal $\mathbf{f}_{2m}$ are the reference model counterparts of those signals in Eq. (10) for the vehicle body. The control force $\mathbf{u}_m$ should be properly determined so that the reference model dynamics be the desired one for the vehicle body. In the present work, the Optimal Control approach was considered for determining the control force of the reference model. The following performance index, that trades-off ride comfort versus suspension deflections, while maintaining constraints on the control effort, was adopted

$$J_m = \lim_{T\to\infty}\frac{1}{T}\int_0^T \left\{ r_1\left(\ddot{q}_{CGm}\right)^2 + r_2(\ddot{\theta}_m)^2 + r_3\left[(q_{1fm} - q_{2f})^2 + (q_{1rm} - q_{2r})^2\right] + r_4(u_{mf}^2 + u_{mr}^2)\right\} dt \tag{13}$$

where r_1, r_2, r_3 and r_4 are weighting coefficients. It is worth noting that the performance index in Eq. (13) and, consequently, the dynamics of the reference model does not depend on the road disturbances z_f and z_r.

Synthesis of the Variable Structure Control Force

Defining the tracking error vector as the difference between the response of the vehicle body $\mathbf{x}_b$ and the response of the reference model $\mathbf{x}_{bm}$, viz.

$$\mathbf{e} = \mathbf{x}_b - \mathbf{x}_{bm} \tag{14}$$

and considering Eqs.(9) and (12), the error dynamics is governed by the following equation

$$\dot{\mathbf{e}} = \mathbf{A}_{bm}\mathbf{e} + \mathbf{f}_k + \mathbf{B}_b\mathbf{u} + \mathbf{f}_m \tag{15}$$

where the signals $\mathbf{f}_k$ and $\mathbf{f}_m$ are defined as follows

$$\begin{aligned} \mathbf{f}_k &= [\mathbf{A}_b - \mathbf{A}_{bm}]\,\mathbf{x}_b + \mathbf{B}_b\mathbf{f}_2 - \mathbf{B}_{bm}\,(\mathbf{u}_m + \mathbf{f}_{2m}) \\ \mathbf{f}_m &= \mathbf{B}_b\left(\mathbf{f}_p + \mathbf{f}_\phi\right) \end{aligned} \tag{16}$$

Its worth noting that the signal $\mathbf{f}_k$ is a known one, since it is composed of system nominal matrices, reference model matrices and known signals. The signal $\mathbf{f}_m$, on the other hand, represents an unknown matched disturbance, associated with unmodeled dynamics, through $\mathbf{f}_\phi$, and parameter uncertainties, through $\mathbf{f}_p$, which is defined in Eq. (11).

The sliding surface S is defined in the error space as follows

$$\mathsf{S} = \{\mathbf{e} \in \mathbf{R}^4 / \ \mathbf{s} = \mathbf{0}\} \tag{17}$$

where $\mathbf{s}$ is an error dependent switching function defined as

$$\mathbf{s} = \mathbf{S}\mathbf{e} \tag{18}$$

where sliding surface matrix $\mathbf{S} \in I\!R^{2\times 4}$ is a design matrix of full rank and it is partitioned as

$$\mathbf{S} = [\mathbf{S}_1 \quad \mathbf{S}_2] \tag{19}$$

where $\mathbf{S}_1 \in I\!R^{2\times 2}$ and $\mathbf{S}_2 \in I\!R^{2\times 2}$. For the existence and uniqueness of the sliding mode, a necessary condition is that the matrix $\mathbf{S}_2$ be nonsigular (Edwards and Spurgeon, 1998).

During the sliding mode, the error dynamics is constrained to the surface S, defined in Eq. (17), and it is given by

$$\dot{\mathbf{e}} = \left[\mathbf{I} - \mathbf{B}_b\left(\mathbf{S}\mathbf{B}_b\right)^{-1}\mathbf{S}\right]\mathbf{A}_{bm}\mathbf{e} \tag{20}$$

Therefore, according Eq. (20), during sliding motion, the error dynamics is independent of the control input $\mathbf{u}$ and it is invariant with respect to the matched disturbance $\mathbf{f}_m$. Hence, a reference model and a sliding surface matrix may be properly synthesized in such a way that the error dynamics asymptotically goes to zero, despite the presence of matched unmodeled dynamics and parameter uncertainties.

In can be shown (Stutz, 2005) that the following proposed control law gives sufficient conditions for inducing and maintaining the error dynamics in sliding mode

$$\mathbf{u}(t) = -\left(\mathbf{S}\mathbf{B}_b\right)^{-1}\mathbf{S}\left[\mathbf{A}_{bm}\mathbf{e}(t) + \mathbf{f}_k(t)\right] + \left(\mathbf{S}\mathbf{B}_b\right)^{-1}\Phi\mathbf{s}(t) - \rho(\mathbf{e},t)\left(\mathbf{S}\mathbf{B}_b\right)^{-1}\frac{\mathbf{P}_2\mathbf{s}(t)}{\|\mathbf{P}_2\mathbf{s}(t)\|}; \quad \text{for} \quad \mathbf{s}(\mathbf{e}(t)) \neq 0 \tag{21}$$

where $\Phi \in I\!R^{2\times 2}$ is an arbitrary matrix whose eigenvalues have negative real parts, $\mathbf{P}_2$ is a symmetric positive definite matrix satisfying the Lyapunov equation

$$\mathbf{P}_2\Phi + \Phi^T\mathbf{P}_2 = -\mathbf{I} \tag{22}$$

and $\rho(\mathbf{e},t)$ is a modulation function, which must satisfy the inequality

$$\rho(\mathbf{e},t) \geq \|\mathbf{S}_2\|\ \|\bar{\mathbf{f}}_m\| + \eta \tag{23}$$

where $\|\cdot\|$ is the norm of $(\cdot)$, η is an arbitrary positive constant, $\mathbf{S}_2$ is given in Eq. (19) and $\bar{\mathbf{f}}_m$ is the projection of $\mathbf{f}_m$ into the range space of $\mathbf{B}_b$. It is worth noting that the modulation function may also be chosen as a constant value, however, in this case, only a local stability of the error dynamics can be proven.

Due to its semi-active nature, the MR dampers are not able to perform the control force given by Eq. (21). Besides, only the input voltages to the current drivers of the MR dampers can be directly controlled. Hence, to induce the MR dampers to generate approximately a desired control force, the Clipped-Control approach (Jansen and Dyke, 1999) was considered and the input voltages V_f and V_r to the front and rear dampers, respectively, are given by

$$\mathbf{V} = V_{max}H\left[(\mathbf{u} - \mathbf{u}_{MR})\mathbf{u}_{MR}\right] \tag{24}$$

where $\mathbf{V}^T = [V_f \quad V_r]$, V_{max} is the maximum applied voltage, $\mathbf{u}_{MR}$ is the force provided by the MR dampers, $\mathbf{u}$ is the desired control force and $H(\cdot)$ is the unit step function.

Table 1 – Nominal parameters of the half-vehicle model, MR dampers and seat-driver subsystem.

m_1	705 kg	J_{CG}	945 kgm^2
m_{2f}	50 kg	m_{2r}	50 kg
d_{1f}	1560 Ns/m	d_{1r}	1309 Ns/m
k_{1f}	24 kN/m	k_{1r}	16.8 kN/m
d_{2f}	0 Ns/m	d_{2r}	0 Ns/m
k_{2f}	250 kN/m	k_{2r}	250 kN/m
a_1	1.30 m	a_2	1.22 m
b_1	3.58 m	b_2	1.06 m

c_{1a}	14649 Ns/m	c_{0a}	784 Ns/m
c_{1b}	34622 $Ns/(Vm)$	c_{0b}	1803 $Ns/(Vm)$
k_1	840 N/m	k_0	3610 N/m
α_a	12441 N/m	β	2059020 m^{-2}
α_b	38430 $N/(Vm)$	γ	136320 m^{-2}
$\mathscr{A}$	58 N/m	n	2
u_0	20,6 N	η_v	190 s^{-1}

m_{d1}	6,7 kg	k_{d1}	50210 N/m	d_{d1}	276 Ns/m
m_{d2}	33,4 kg	k_{d2}	35776 N/m	d_{d2}	761 Ns/m
m_{d3}	10,7 kg	k_{d3}	38374 N/m	d_{d3}	458 Ns/m

MR-OPTIMAL VEHICLE SUSPENSION SYSTEM

For comparison purposes, a MR vehicle suspension system based on the Optimal Control approach is also considered in this work. The following performance index, which trades-off ride comfort versus tyre deflections, while maintaining constraints on suspension deflections and control efforts, was adopted

$$J = \lim_{T\to\infty} \frac{1}{T} \int_0^T \Big\{ \rho_1 (\ddot{q}_{CG})^2 + \rho_2 (\ddot{\theta})^2 + \rho_3 \left[(q_{1f} - q_{2f})^2 + (q_{1r} - q_{2r})^2 \right] + \\ + \rho_4 \left[(q_{2f} - z_f)^2 + (q_{2r} - z_r)^2 \right] + \rho_5 (u_f^2 + u_r^2) \Big\} dt \tag{25}$$

where ρ_1, ρ_2, ρ_3, ρ_4 and ρ_5 are weighting coefficients and the front and rear road disturbances z_f and z_r can be modeled as the output of a first order filter (Hać et al., 1996a). However, since the rear road disturbance is the time-delayed front disturbance, one has

$$\dot{z}_f + (a\mathscr{V}) z_f = \xi_f \qquad ; \qquad z_r(t) = z_f(t - (a_1 + a_2)/\mathscr{V}) \tag{26}$$

where $\mathscr{V}$ is the vehicle velocity, a is a parameter depending on the road surface quality, ξ is a white noise process with intensity $W = 2\sigma^2 a\mathscr{V}$, where σ^2 is the variance of the road irregularities, and $(a_1 + a_2)$ is the distance between the front and rear wheels.

The optimal control force is given by

$$\mathbf{u} = -\mathbf{G}_a \mathbf{x}_a \tag{27}$$

where $\mathbf{G}_a$ is the control gain and $\mathbf{x}_a^T = [\mathbf{x} \quad z_f \quad z_r]$ is the augmented state vector, with $\mathbf{x}$ given by Eq. (2). It is worth noting that the optimal control force given by Eq. (27) requires the knowledge of the road disturbances z_f and z_r.

Once again, to induce the MR dampers to generate approximately the optimal control force, given by Eq. (27), the input voltages to their current drivers are given by Eq. (24).

NUMERICAL ANALYSES

In order to assess the performance of the MR suspensions, numerical analyses considering the half-vehicle model were carried out. Despite not have been considered for the synthesis of the suspensions, the seat-driver subsystem, depicted in Fig. 3, was also considered for the performance assessment. The nominal parameters of the vehicle model, MR dampers and seat-driver subsystem are given in Table 1.

The MR suspensions were obtained just replacing the passive dampers of the vehicle model with the MR ones. The input voltages to the current driver of these dampers was selected according Eq. (24) with the maximum voltage $V_{max} = 2V$.

Steady-state disturbances, induced by paved and asphalt roads, and a transient disturbance, induced by an impact bump, were considered in the analyses. Figure 5 depicts the road induced disturbances at the front wheel for a vehicle speed $\mathscr{V} = 20m/s$. The steady-state disturbances were obtained from Eq. (26), with $a = 0.45\ m^{-1}$ and $\sigma^2 = 3{\cdot}10^{-4}\ m^2$ for the paved road, and with $a = 0.15\ m^{-1}$ and $\sigma^2 = 9{\cdot}10^{-6}\ m^2$ for the asphalt road.

The MR-VSC suspension was obtained as follows. The nominal parameters of the vehicle were adopted as the ones of the reference model and the weighting coefficients for deriving the control force of the reference model were chosen as

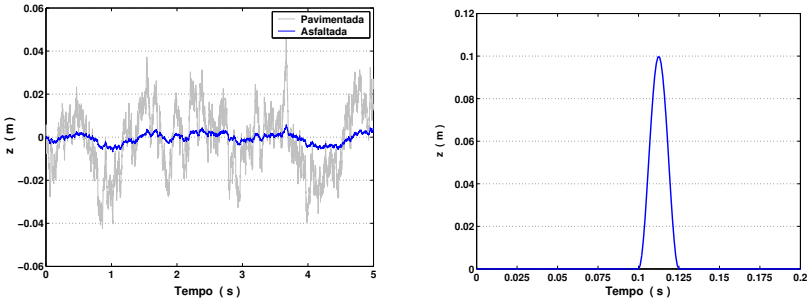

Figure 5 – Road induced disturbances at the front wheel for a vehicle speed $\mathscr{V} = 20m/s$.

$r_1 = 1$, $r_2 = 2$, $r_3 = 2.35 \cdot 10^4$ and $r_4 = 10^{-6}$. The sliding surface S was defined adopting $\mathbf{S}_1$ and $\mathbf{S}_2$ as identity matrices. The same for matrix Φ of the desired control law in Eq. (21), which resulted, from Eq. (22), in $\mathbf{P}_2 = 0.5\mathbf{I}$. The modulation function was adopted as $\rho = 3$. Finally, the input voltages was selected according Eq. (24).

The MR-Optimal suspension was obtained considering the weighting coefficients $\rho_1 = 1$, $\rho_2 = 2$, $\rho_3 = 2 \cdot 10^3$, $\rho_4 = 2.5 \cdot 10^4$ and $\rho_5 = 10^{-6}$. The input voltages was selected according Eq. (24) with the desired control force given by Eq. (27). It must be emphasized here that the implementation of the MR-Optimal suspension, according to Eqs. (26) and (27), requires a knowledge of the road induced disturbances z_f and z_r.

For comparison purposes, active suspensions capable of providing integrally the control forces given in Eqs. (21) and (27) were also considered. These suspensions were named VSC and LQG, respectively. It is worth noting that these are ideal suspensions, since the dynamics of their actuators were not taken into account. The control parameters for these suspensions were kept the same of their MR counterparts.

In the results that follows, the steady-state performance of the suspensions were assessed in terms of *rms*, maximum and average deviation values of the displacement and acceleration of point C (driver position in Fig. 3); acceleration of point B and deflections of the front suspension and tyre. The average deviation d_{rms} of a signal is defined as the *rms* value of its time derivative and it is supposed to provide some information about the frequency content of the signal. The performance indices were computed for a simulation time $T = 10s$.

The performance of the suspensions, relative to the passive one, for the rigid body vehicle and the disturbance induced by the paved road is given in Tab. 2. From this, one can clearly see that all considered suspensions greatly improved on ride comfort, which is related to the performance indices associated with the acceleration of points B and C. With respect to the acceleration of point B, the MR suspensions presented a performance comparable to that of the active ones. The suspensions also improved on the performance indices associated with the displacement of point C, specially the VSC one, whose performance was greatly superior to that of the others suspensions. All considered suspensions presented relatively great d_{rms} values of the deflections, indicating a possibility of greater amplitudes in the high frequency components of these signals. Performance indices associated with the tyre deflections are also shown in Tab. 2.

Table 2 – Performance relative to the passive suspension one for the rigid body vehicle and the paved road disturbance.

		Suspension			
		LQG	VSC	MR-LQG	MR-VSC
q_C	rms	0,54	0,29	0,90	0,81
	max	0,52	0,30	0,89	0,87
	d_{rms}	0,47	0,35	0,88	0,79
$\ddot{q}_C$	rms	0,57	0,58	0,76	0,76
	max	0,58	0,59	0,68	0,67
	d_{rms}	0,72	0,71	0,70	0,70
$\ddot{q}_B$	rms	0,72	0,70	0,74	0,71
	max	0,70	0,67	0,66	0,69
	d_{rms}	0,77	0,70	0,74	0,74
$(q_{1f} - q_{2f})$	rms	1,06	1,06	1,14	1,14
	max	1,08	1,03	1,11	1,14
	d_{rms}	1,38	1,41	1,42	1,47
$(q_{2f} - z_f)$	rms	1,28	1,31	1,27	1,31
	max	1,08	1,12	1,03	1,08
	d_{rms}	1,03	1,03	1,03	1,03

For the rigid body vehicle, all suspensions also presented a great improvement on the ride comfort obtained by the passive suspension when considering the asphalt road and the impact bump (Stutz, 2005).

Despite have not been considered for the synthesis of the suspensions, the flexibility of the vehicle body yield struc-

tural vibrations that may result in a great performance drop (Hać et al., 1996a, 1996b). This is due to the subjective discomfort from the direct exposure to high frequency vibrations or noise. Hence, due to the control-structure interaction, accounting for the flexibility of the vehicle body, in the performance assessment of active and MR suspensions systems, is a fundamental concern. However, these structural vibrations may present little increment on the *rms* values of acceleration signals, which are standard indices of ride comfort. Hence, as the average deviation d_{rms} is supposed to provide some information about the frequency content of the signals, it will be used here as a complementary index of ride comfort.

For taking the flexibility of the vehicle body into account, the Finite Element Method (Reddy, 1984) was considered. The vehicle body was modeled as an uniform beam and 10 finite Euler-Bernoulli beam elements were used for its discretization. Then, the bending stiffness EI of the body was adjusted so that the vehicle first natural frequency fitted the corresponding one given by Hać et al. (1996a). The other parameters are given in Tab. 1.

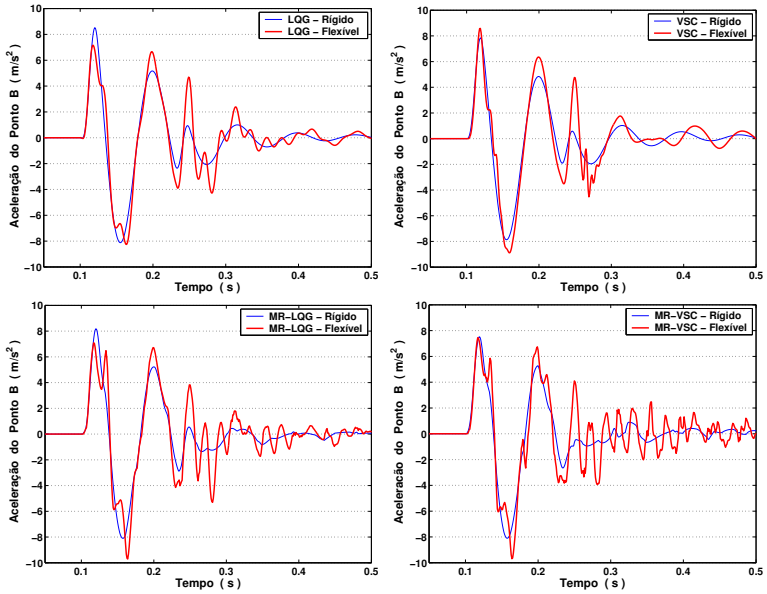

Figure 6 – Acceleration of point B at the rigid and flexible vehicles with the active and MR suspensions for the impact bump.

The influence of the vehicle body flexibility on the transient performance of the suspensions is depicted in Fig. 6. This figure presents the acceleration of point B, due to the impact bump, at the rigid and flexible vehicles with the active and MR suspensions. From Fig. 6, one can clearly note the influence of the body flexibility on the oscillation amplitudes and on the presence of high frequency components in the acceleration of point B at the flexible vehicle. The MR suspensions presented greater performance drops, due to the flexibility of the vehicle body, than the active ones. For those suspensions, especially the VSC-MR one, the high frequency vibrations lasted for longer times and presented higher amplitudes. It is worth noting that the active VSC suspension was able to quickly suppress the high frequency vibrations in the acceleration of point B.

Table 3 presents the the performance of the suspensions, relative to the passive one, for the flexible body vehicle and the disturbance induced by the paved road. In spite of the flexibility have not been considered for the synthesis of the suspensions, it can be seen that all suspensions greatly improved on ride quality. The performance indices associated with the acceleration of point C along with the *rms* and maximum values of the acceleration of point B were greatly improved. The suspensions also improved on the performance indices associated with the displacement of point C. The active suspensions presented a great improvement on these indices, specially the VSC one, whose performance, as in the rigid body case, was greatly superior to that of the others suspensions. It is worth noting that the MR suspensions presented maximum values of the front deflections significantly greater than that of the passive suspension. All suspensions presented relatively great d_{rms} values of the deflections.

The performance of the suspensions, relative to the passive one, for the flexible vehicle and the disturbance induced by the asphalt road is given in Tab. 4. From the presented results, it can be clearly seen that the active suspensions greatly improved on ride comfort. The MR suspensions also presented great improvements on the *rms* and maximum values of the acceleration of point C. With respect to the acceleration of point B, among the MR suspensions, only the MR-LQG presented an improvement on the *rms* and maximum values. The MR suspensions presented higher d_{rms} values of the acceleration of points B and C, especially the MR-VSC. However, the low *rms* value of the tyre deflection for this suspension indicates that a better performance on ride quality may be achieved. All suspensions improved on the performance indices associated with the displacement of point C.

Table 3 – Performance relative to the passive suspension one for the flexible body vehicle and the paved road disturbance.

		Suspension			
		LQG	VSC	MR-LQG	MR-VSC
q_C	rms	0.53	0.29	0.90	0.81
	max	0.53	0.31	0.95	0.91
	d_{rms}	0.46	0.34	0.89	0.79
$\ddot{q}_C$	rms	0.58	0.61	0.78	0.78
	max	0.59	0.60	0.68	0.65
	d_{rms}	0.72	0.73	0.72	0.74
$\ddot{q}_B$	rms	0.71	0.72	0.74	0.73
	max	0.68	0.67	0.79	0.78
	d_{rms}	1.02	0.54	0.93	0.96
$(q_{1f} - q_{2f})$	rms	0.97	0.93	1.12	1.09
	max	1.06	0.93	1.22	1.24
	d_{rms}	1.38	1.27	1.42	1.48
$(q_{2f} - z_f)$	rms	1.27	1.20	1.27	1.31
	max	1.07	1.05	1.03	1.12
	d_{rms}	1.03	1.02	1.03	1.03

Table 4 – Performance relative to the passive suspension for the flexible body vehicle and the asphalt road disturbance.

		Suspension			
		LQG	VSC	MR-LQG	MR-VSC
q_C	rms	0.61	0.30	0.80	0.75
	max	0.58	0.30	0.82	0.79
	d_{rms}	0.49	0.31	0.74	0.65
$\ddot{q}_C$	rms	0.54	0.53	0.74	0.77
	max	0.58	0.50	0.69	0.65
	d_{rms}	0.71	0.73	1.05	1.25
$\ddot{q}_B$	rms	0.69	0.68	0.88	1.00
	max	0.69	0.61	0.93	1.12
	d_{rms}	0.98	0.55	1.95	2.25
$(q_{1f} - q_{2f})$	rms	0.94	1.02	0.94	0.87
	max	0.92	1.07	1.00	0.96
	d_{rms}	1.36	1.25	1.30	1.17
$(q_{2f} - z_f)$	rms	1.25	1.18	1.18	1.08
	max	1.11	1.07	1.08	1.09
	d_{rms}	1.03	1.02	1.02	1.01

From the results presented in this section, one can note a drop in the performance of the suspensions due to the flexibility of the vehicle body. The greater drops were presented by the MR suspensions, mainly for the impact bump and the asphalt road. However, the Clipped-Control algorithm used in the MR dampers may result in a high frequency control force, which may excite the flexible modes of the vehicle body, contributing to a performance drop. Besides, if the road induced disturbances are not sufficient to yield the MR fluid through the damper valves, the dampers will behave as rigid elements, between the vehicle body and the wheels, and, in this case, all of the vibration energy will be transmitted by the suspension.

CONCLUDING REMARKS

The synthesis of a magneto-rheological vehicle suspension system based on the Variable Structure Control approach was considered in the present work. A half-vehicle model with rigid body was considered for the suspension synthesis. The performance of the suspension was assessed through numerical analyses. In these analyses, phenomenological models for the MR dampers and for the seat-driver subsystem along with the flexibility of the vehicle body were taken into account. For comparison purposes, the following suspensions were also considered: MR-LQG, active LQG and active VSC. For the rigid body vehicle and the disturbance induced by the paved road, all the considered suspensions greatly improved on the ride quality obtained by the standard passive suspension. In general, the active suspensions outperformed the MR ones. However, it must be emphasized that, differently for the MR dampers, the dynamics of the active actuators was not considered in the numerical analyses. All the suspensions, specially the MR ones, presented a drop in their performances when the flexibility of the vehicle body was taken into account. The greater performance drops were observed for the impact bump and the asphalt road disturbances. Therefore, considering these disturbances and the MR suspensions, the improvement on the ride comfort predicted by the rigid vehicle model is not verified. For the MR suspensions, the discontinuity of the input voltages to the current drivers, determined from the Clipped-Control algorithm, along with the visco-plastic behavior of the MR fluids, may have contributed for a greater performance drop. From the numerical results presented, one can observe that the performance of a MR suspension is greatly dependent on the control approach, the disturbance intensity and the vehicle model considered.

REFERENCES

Carlson, J.D. and Spencer Jr., B.F., 1996, "Magneto-Rheological Fluid Dampers: Scalability and Design Issues for Application to Dynamic Hazard Mitigation", Proc. 2nd International Workshop on Structural Control, Hong Kong, pp. 99–109.

Edwards, C. and Spurgeon, S.K., 1998, "Sliding Mode Control: Theory and Applications", Ed. Taylor and Francis, London, UK.

Hać, A., Youn, I. and Chen, H.H., 1996a, "Control of Suspensions for Vehicles with Flexible Bodies - Part I: Active Suspensions", Trans. of ASME, Journal of Dynamic Systems, Measurement and Control, Vol. 118, pp. 508-517.

Hać, A., Youn, I. and Chen, H.H., 1996b, "Control of Suspensions for Vehicles with Flexible Bodies - Part II: Semi-Active Suspensions", Trans. of ASME, J. of Dynamic Systems, Measurement and Control, Vol. 118, pp. 518-525.

Hrovat, D., 1997, "Survey of Advanced Suspension Developments and Related Optimal Control Applications", Automatica, Vol. 33, No. 10, pp. 1781–1817.

Jansen, L.M. and Dyke, S.J., 1999, "Semi-Active Control Strategies for MR Dampers: A Comparative Study", ASCE Journal of Engineering Mechanics, Vol. 126, No. 8, pp. 795–803.

Reddy, J.N., 1984, "An introduction to the Finite Element Method", Ed. McGraw-Hill.

Sharp, R.S. and Hassan, S.A., 1986, "An Evaluation of Passive Automotive Suspension Systems with Variable Stiffness and Damping Parameters", Vehicle System Dynamics, Vol. 15, pp. 335–350.

Spencer Jr., B.F., Dyke, S.J., Sain, M.K. and Carlson, J.D., 1996, "Phenomenological Model of a Magneto-Rheological Damper", Journal of Engineering Mechanics, Vol. 123, No. 3, pp. 230–238.

Stutz, L.T., 2005, "Synthesis and Analysis of a Magneto-Rheological Suspension Based on the Variable Structure Control Approach", D.Sc. Thesis, Mechanical Engineering Department, COPPE/UFRJ, Brazil. In Portuguese.

Stutz, L.T. and Rochinha, F.A., 2005, "A Comparison of Control Strategies for Magnetorheological Vehicle Suspension Systems", Proceedings of the XI DINAME, Minas Gerais, Brazil.

Wei, L. and Griffin, M.J., 1998, "Mathematical Models for the Apparent Mass of Seated Human Body Exposed to Vertical Vibration", Journal of Sound and Vibration, Vol. 212, No. 5, pp. 855–874.

Yao, G.Z., Yap, F.F., Chen, G., Li, W.H. and Yeo, S.H., 2002, "MR Damper and its Application for Semi-Active Control of Vehicle Suspension System", Mechatronics, Vol. 12, pp. 963973.

Yokoyama, M., Hedrick, J.K. and Toyama, S., 2001, "A Model Following Sliding Mode Controller for Semi-Active Suspension Systems with MR Dampers", Proc. of the American Control Conference, Arlington, pp. 2652–2657.

RESPONSIBILITY NOTICE

The author(s) is (are) the only responsible for the printed material included in this paper.